JJMIE

Volume 16, Number 3, June. 2022
ISSN 1995-6665
Pages 343 - 352

Jordan Journal of Mechanical and Industrial Engineering

Research on Robust Control of Automobile Anti-lock Braking System Based on Road Recognition

Gengxin Qi [1, *], Xiaobin Fan[1], Shuaiwei Zhu[1], Xinbo Chen[2], Pan Wang[1], Hao Li[1]

[1]School of Mechanical and Power Engineering, Henan Polytechnic University, Jiaozuo 454000, P.R. China

[2]China North Vehicle Research Institute, Beijing, 100072, China.

Received 23 Nov 2021 Accepted 23 Mar 2022

Abstract

Automobile anti-lock braking system (ABS) is an important component of vehicle active safety control system and is widely used in various automobiles. In the car braking process, the car equipped with ABS can effectively shorten the braking distance, and avoid vehicle side-slip, etc., ensuring the braking performance and driving safety of the vehicle. In order to further improve the performance and robustness of automobile ABS, a robust ABS control method based on road recognition is proposed for the current ABS control method. Based on the fuzzy logic control method, the road surface adhesion coefficient is estimated to realize the road surface recognition, and the optimal slip rate is dynamically obtained. According to the slip rate, a robust controller of ABS is designed. The simulation results show that the robust controller of ABS has good control effect and robustness and can estimate the road adhesion coefficient in real time.

Keywords: Automobile anti-lock braking system, vehicle active safety system, tire/road adhesion coefficient, fuzzy logic algorithm, robust controller.

1. Introduction

With the development of the automobile industry and the increase of car ownership, the rate of road traffic accidents is also increasing. One of the main factors which causes a lot of traffic accidents and affects traffic safety is driving the car without road information acquisition. To assure the stability of the vehicle under the condition of the critical, anti-lock braking system (ABS), acceleration slip regulation (ASR) and electronic stability program (ESP) have become a necessity for modern car active safety control system [1-2]. ABS can automatically adjust the wheel braking torque to avoid the phenomenon of lock and slip in the braking process. The vehicle is controlled near the optimal slip rate to ensure that the wheel braking has sufficient ground braking force and large lateral force, to improve the directional stability and steering maneuverability of the vehicle, and shorten the braking distance [3].

The control method is the core technology of ABS. Most mature ABS control methods are based on the threshold of speed increment and decrease and the reference slip rate. Although simple and practical, there are some difficulties in debugging and road identification. At present, a variety of ABS control methods with the slip rate as the control target have become the research hotspot. This kind of control method is in the form of continuous quantity control to keep the slip rate optimal and stable during braking. The main control algorithms used in the study of ABS control based on slip rate include logic threshold [4-5], Proportional Integral Derivative (PID) [6-7], fuzzy neural network [8-9], sliding mode control [10-11], optimal control [12-13] and other algorithms. Fu *et al.* [14] took a dangerous goods transport vehicle as the research object and took the slip rate as the control objective, designed the ABS system with three control strategies of Bang-Bang control PID control and adaptive fuzzy PID control, and carried out simulation analysis. Emam *et al.* [15] designed the proportional integral derivative (PID) and fuzzy logic control (FLC) control algorithms based on the optimal slip rate, and carried out simulation tests on rough dry and wet roads, and the results showed that the fuzzy logic algorithm had better control effect. Xu [16] designed a PID control algorithm and a fuzzy PID control algorithm based on the slip rate for anti-lock braking of new energy vehicles. Through MATLAB simulation experiments, it can be proved that the response speed and control precision of the fuzzy PID control algorithm, stability and security can be effectively improved. In order to make full use of the road adhesion ability to improve the braking safety of electric vehicles. On the basis of analyzing the shortcomings of the traditional control algorithm of ABS, He *et al.* [17] proposed a fuzzy immune adaptive PID control algorithm combining the biological immune principle and the adaptive ability of fuzzy logic reasoning. This method had the characteristics of small overshoot, fast response, short braking distance and strong anti-interference ability. Jia *et*

* Corresponding author e-mail: 1394599023@qq.com.

al. [18] proposed a kind of ABS adaptive fuzzy PID controller. According to the simulation test, the performance of ABS controlled by adaptive fuzzy PID had been greatly improved compared with the conventional braking system. It had the characteristics of online self-tuning parameters, and had good stability adaptability and robustness. Mao *et al.* [19] proposed an ABS fuzzy immune PID controller. By comparison with traditional PID control through simulation tests, the fuzzy PID free control algorithm had more advantages and higher security in anti-lock braking control. At present, there are more researches on adaptive control or neural control. Yao *et al.* [20] proposed a kind of ADRC of automobile anti-lock braking system, built automobile dynamics model, brake system model, tire model and slip rate model and other major models, designed ABS second-order nonlinear ADRC controller based on slip rate and used MATLAB/Simulink software to control based on active disturbance rejection control (ADRC). Wang *et al.* [21] proposed an electric vehicle anti-lock braking system control method based on radial basis function neural network road recognition. The slip rate was used as the target parameter, and an ABS control strategy combining fuzzy control and predictive control was designed with this, and a braking torque distribution strategy was formulated at the same time. Shen *et al.* [22] established a theoretical model of vehicle anti-lock braking system based on optimal control theory, and compared the effect of ordinary braking and ABS control based on optimal control algorithm through simulation analysis. Wu *et al.* [23] proposed the optimal tracking control of the slip rate for the anti-lock braking system of high-speed vehicles under complex road conditions. Similarly, sliding mode control was also the main control algorithm of ABS due to its robustness, but its chattering cannot be eliminated, which seriously affected its performance. In order to eliminate chattering and enhance its performance, Wang *et al.* [24] proposed an ABS sliding mode variable structure control method based on road surface recognition. This method can recognize the road surface based on the road characteristic coefficient method, dynamically obtain the optimal slip rate of the current vehicle, and then carry out sliding mode variable structure control on the vehicle ABS based on the optimal slip rate. Peri *et al.* [25] proposed a minimum variance control based on digital sliding mode. In the proposed control, the minimum variance enabled the digital sliding mode control to be designed only based on the output measurement of ABS, while the sliding mode control increased the robustness of ABS under certain conditions. Chereji *et al.* [26] proposed an antilock braking system based on sliding mode control algorithm, and introduced two kinds of sliding mode control based on Lyapunov sliding mode Controller (LSMC) and Reach law sliding mode controller (RSMC), and introduced the performance of the algorithm and its application in strongly nonlinear antilock braking system. Wang *et al.* [27] proposed an improved optimal sliding mode control method for automobile hydraulic anti-lock braking system to achieve robustness and optimal control performance. Wanaskar *et al.* [28] proposed a robust sliding mode controller based on disturbance observer. In order to verify the robustness of the controller, a braking simulation was carried out on a two-axle vehicle model under dry asphalt pavement with snow cover and changing road conditions. Hossein *et al.* [29] proposed a new prediction-based robust controller for antilock braking system, which can guarantee the stability of antilock braking system under uncertainty.

In view of the current ABS control algorithm, in overcoming the high non-linearity, time variability and parameter uncertainty of ABS control, there are problems such as poor anti-interference ability and poor ability to adapt to parameter changes. The most important problem of ABS controller with slip rate as the control target is the stability of the control, that is, the robustness of the system. To improve the robustness of the system, the ABS robust control based on road surface recognition is proposed in this paper. The method realizes road identification by fuzzy logic control algorithm, estimates road adhesion coefficient in real time, and obtains optimal dynamic slip rate. With slip rate as the control objective, ABS robust controller is designed and compared with the traditional PID control method. In this paper, an eight-degree-of-freedom vehicle model is established as the research object, and then the braking experiment and road identification simulation of the control method are carried out through MATLAB/Simulink software to verify its effectiveness.

2. Vehicle Dynamics Model

2.1. Vehicle Model with Eight Degrees of Freedom

In this paper, the vehicle is simplified as a vehicle model with eight degrees of freedom [30-31]. The vehicle dynamics model is shown in Figure 1, including the transverse motion, longitudinal motion, yaw motion, roll motion, and the rotation motion of four wheels around their respective axes.

The following assumptions are made for the vehicle model:

1. It is assumed that the road surface is relatively smooth, without the vertical and pitching motion of the vehicle in the vertical direction;
2. It is assumed that the origin of the moving coordinate system solidified with the vehicle coincides with the center of mass of the vehicle;
3. Ignore the rolling resistance and air resistance during the movement of tires;
4. It is assumed that each tire has the same mechanical characteristics;
5. It is assumed that the tire angle on the same shaft is the same in the steering process.

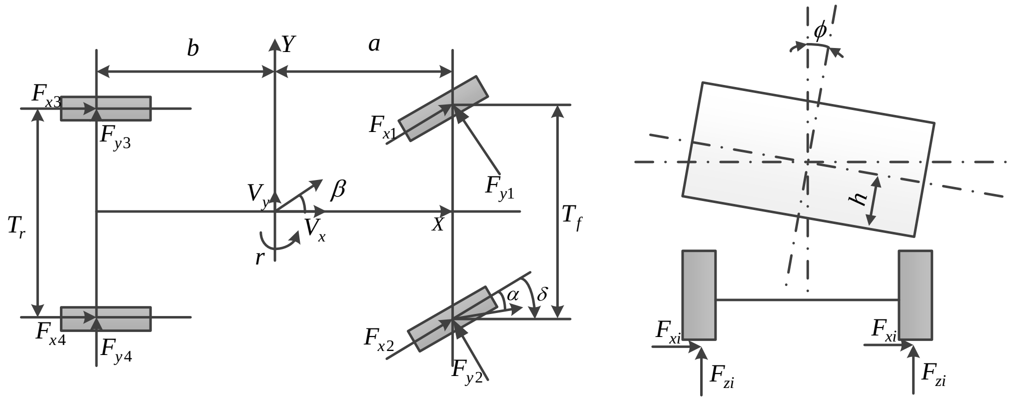

Figure 1. Vehicle dynamics model

Lateral motion：

$$m\left(\dot{v}_y + v_x r\right) = \left(F_{x1} + F_{x2}\right)\sin\delta_{df} + \left(F_{y1} + F_{y2}\right)\cos\delta_{df} + F_{y3} + F_{y4} + m_s h\ddot{\phi} \tag{1}$$

Longitudinal motion：

$$m\left(\dot{v}_x - v_y r\right) = \left(F_{x1} + F_{x2}\right)\cos\delta_{df} - \left(F_{y1} + F_{y2}\right)\sin\delta_{df} + F_{x3} + F_{x4} - m_s h\dot{\phi} r \tag{2}$$

Horizontal pendulum motion：

$$\begin{aligned} I_z\dot{r} = I_{xz}\dot{\phi} + \frac{T_f}{2}\left(F_{x2} - F_{x1}\right)\cos\delta_{df} + \frac{T_f}{2}\left(F_{y1} - F_{y2}\right)\sin\delta_{df} + \frac{T_r}{2}\left(F_{x4} - F_{x3}\right) + \\ a(F_{x1} + F_{x2})\sin\delta_{df} + a(F_{y1} + F_{y2})\cos\delta_{df} - b(F_{y3} + F_{y4}) \end{aligned} \tag{3}$$

Rolling motion:

$$I_x\ddot{\phi} = -K_\phi\phi - C_\phi\phi + m_s gh\sin\delta_{df} + m_s h\left(\dot{v}_y + v_x r\right) \tag{4}$$

Rolling of the wheels：

$$I_{\omega i}\dot{\omega} = T_{di} - F_{xi}R_w - T_{\mu di}\left(i = 1,2,3,4\right) \tag{5}$$

In the formula, m is the mass of vehicle reconditioning, kg; m_s is the sprung mass of the car, kg; v_x and v_y respectively represent the velocities of vehicles along the X and Y direction, m/s; r is the angular velocity of the pendulum, rad/s; $F_{xi}\left(i = 1,...,4\right)$ 、 $F_{yi}\left(i = 1,...,4\right)$ respectively represent the longitudinal force and transverse force of the tire, N; $T_{\mu di}\left(i = 1,...,4\right)$ is dynamic output braking torque, $N \cdot m$; $T_{di}\left(i = 1,...,4\right)$ is the wheel driving torque, $N \cdot m$; a, b respectively represent the distance from the center of mass to the front and back axis, m; h is height of the center of mass, m; T_f and T_r respectively represent the front and rear wheel spacing, m; δ_{df} is driver angle input, rad; I_x, I_z and I_{xz} represent the moment of inertia and product of inertia of the sprung mass around the X and Z axes, respectively, $kg \cdot m^2$; ϕ, $\dot{\phi}$ and $\ddot{\phi}$ respectively represent the body roll angle, roll angular velocity, and roll angular acceleration, rad, rad/s, and rad/s^2; K_ϕ is the Suspension roll stiffness, $N \cdot m/rad$; C_ϕ is suspension damping, $N \cdot m \cdot s/rad$; $I_{wi}\left(i = 1,...,4\right)$ represents rotational inertia of the wheels and their components, $kg \cdot m^2$; R_w is wheel radius, m; $\omega_i\left(i = 1,...,4\right)$ is the angular velocity of the wheel, rad/s.

2.2. Brake system model

When braking, the brake hydraulic transmission system can be simplified into a solenoid valve link, a first-order inertia link and an integral link. The simplified model transfer function is shown in formula (6) [3]:

$$G(s) = \frac{K}{s \cdot (T_p s + 1)} \tag{6}$$

In the formula, s is the Laplace operator; K is the system gain; T_p is the time constant.

2.3. Tire Model

Considering the nonlinearity in the process of tire motion, the Dugoff model [32] is adopted to analyze the force on the tire.

Longitudinal force of the tire is given as:

$$F_{xi} = C_x \frac{\lambda}{1+\lambda} f\left(S_i\right) \tag{7}$$

Lateral force of the tire is given as:

$$F_{yi} = C_y \frac{\tan\alpha_i}{1+\lambda} f\left(S_i\right) \tag{8}$$

$$S_i = \frac{\mu F_{zi}\left(1+\lambda\right)}{2\sqrt{\left(C_x\lambda\right)^2+\left(C_y \tan\alpha_i\right)^2}} \tag{9}$$

$$f\left(S_i\right)=\begin{cases}\left(2-S_i\right)S_i & \left(S_i \le 1\right)\\ 1 & \left(S_i > 1\right)\end{cases} \tag{10}$$

In the formula, C_x is longitudinal stiffness of tire, $N\cdot m/rad$; S_i is the parameter set in the middle. λ is the longitudinal slip of tire; C_y is lateral stiffness of tire, $N\cdot m/rad$; $\alpha_i\left(i=1,...,4\right)$ is wheel side slip angle, rad. μ is the longitudinal road adhesion coefficient.

2.4. Vertical Load of the Wheel

The vertical load of each wheel is given as:

$$F_{z1}=\frac{mgb}{2\left(a+b\right)}-\frac{mh\dot{v}_x}{2\left(a+b\right)}-\frac{mh\dot{v}_y b}{\left(a+b\right)T_f}-\frac{(K_{\phi f}\phi+C_{\phi f}\dot{\phi})}{T_f} \tag{11}$$

$$F_{z2}=\frac{mgb}{2\left(a+b\right)}-\frac{mh\dot{v}_x}{2\left(a+b\right)}+\frac{mh\dot{v}_y b}{\left(a+b\right)T_f}+\frac{(K_{\phi r}\phi+C_{\phi r}\dot{\phi})}{T_f} \tag{12}$$

$$F_{z3}=\frac{mga}{2\left(a+b\right)}+\frac{mh\dot{v}_x}{2\left(a+b\right)}-\frac{mh_{cg}\dot{v}a}{\left(a+b\right)T_r}-\frac{(K_{\phi r}\phi+C_{\phi r}\dot{\phi})}{T_r} \tag{13}$$

$$F_{z4}=\frac{mga}{2\left(a+b\right)}+\frac{mh\dot{v}_x}{2\left(a+b\right)}+\frac{mh\dot{v}_y a}{\left(a+b\right)T_r}-\frac{(K_{\phi r}\phi+C_{\phi r}\dot{\phi})}{T_r} \tag{14}$$

In the formula, $C_{\phi f}$ is front suspension roll damping, $N\cdot m\cdot s/rad$; $C_{\phi r}$ is rear suspension roll damping, $N\cdot m\cdot s/rad$; $K_{\phi f}$ is front suspension roll stiffness, $N\cdot m/rad$; $K_{\phi r}$ is rear suspension roll stiffness, $N\cdot m/rad$.

2.5. Each Wheel Side Slip Angle and Speed of the Wheel Center

Each wheel side slip angle and speed of the wheel center are given as:

$$\alpha_1 = \delta_{df} - arctan\left(\frac{v_y + ar}{v_x - 0.5T_f r}\right) \tag{15}$$

$$\alpha_2 = \delta_{df} - arctan\left(\frac{v_y + ar}{v_x + 0.5T_f r}\right) \tag{16}$$

$$\alpha_3 = -arctan\left(\frac{v_y - br}{v_x - 0.5T_r r}\right) \tag{17}$$

$$\alpha_4 = -arctan\left(\frac{v_y - br}{v_x + 0.5T_r r}\right) \tag{18}$$

$$v_{\omega 1}=\left(v_x-0.5T_f r\right)\cos\delta_{df}+\left(v_y+ar\right)\sin\delta_{df} \tag{19}$$

$$v_{\omega 2}=\left(v_x+0.5T_f r\right)\cos\delta_{df}+\left(v_y+ar\right)\sin\delta_{df} \tag{20}$$

$$v_{\omega 3}=\left(v_x-0.5T_r r\right) \tag{21}$$

$$v_{\omega 4}=\left(v_x+0.5T_r r\right) \tag{22}$$

2.6. Slip Rate Calculation

$$\lambda=\frac{v_x-v_{\omega i}}{v_x}\times 100\%=\left(1-\frac{\omega_i R_w}{v_x}\right)\times 100\% \qquad \left(i=1,2,3,4\right) \tag{23}$$

In the formula, $v_{\omega i}\left(i=1,\cdots,4\right)$ is the velocity of the wheel center, m/s.

3. H_∞ Robust Control Design of Automobile Anti-lock Braking System

3.1. ABS System Equation

To reduce the complexity of the algorithm, a single-wheel vehicle model is used for algorithm research based on the D'Alembert principle. The model is simplified as two degrees of freedom of the vehicle body in the driving direction and the wheel around the spindle direction. The vehicle dynamics model is shown in Figure 2.

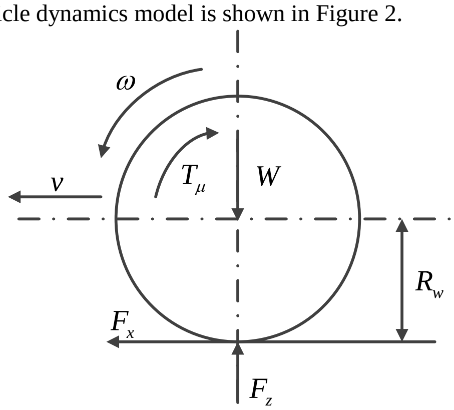

Figure 2. Two-degree-of-freedom vehicle dynamics model

$$M\dot{v}_x=-F_{xb} \tag{24}$$

$$I_\omega\dot{\omega}=F_{xb}R_w-T_{\mu d} \tag{25}$$

$$\mu=\frac{F_{xb}}{F_z} \tag{26}$$

In the formula, M is the mass of the car allocated to the wheels, kg; F_{xb} is the ground braking force, N.

Assuming that the change of vehicle speed is less than that of wheel speed during anti-lock braking, the definition of slip ratio is derived as follows:

$$\dot{\lambda}=-\frac{R_w}{v_x}\dot{\omega}+\frac{\omega R_w}{v_x^{\ 2}}\dot{v}_x \tag{27}$$

To facilitate the mathematical processing and simulation research in the control process, the brake is assumed to be an ideal component in the calculation, and its nonlinear characteristics are considered weak and the impact of its hysteresis is ignored. Therefore, the brake simplified equation is:

$$T_{\mu d}=C\cdot p \tag{28}$$

In the formula, C is the brake efficiency factor; p is the brake pressure.

Regarding the braking pressure and wheel slip rate of the anti-lock brake system as state variables, the mathematical model of the ABS system is simplified by referring to the model simplification method of the literature [22]. The state equation of the system is:

$$\begin{bmatrix} \dot{p} \\ \dot{\lambda} \end{bmatrix} = \begin{bmatrix} -\frac{1}{T_p} & 0 \\ \frac{CR_w}{I_\omega v} & \frac{F_x}{Mv} \end{bmatrix} \begin{bmatrix} p \\ \lambda \end{bmatrix} + \begin{bmatrix} \frac{1}{T_p} \\ 0 \end{bmatrix} \tag{29}$$

The output equation Y is:

$$Y = \begin{bmatrix} 0 & 1 \end{bmatrix} \begin{bmatrix} p \\ \lambda \end{bmatrix} \tag{30}$$

3.2. H_∞ Robust Control Design

The standard H_∞ control problem is shown in Figure 3. The principle is to design a feedback controller $K(s)$ to optimize the infinite norm of performance indicators. That is， $K(s)$ minimizes the H_∞ norm of the objective function P while stabilizing the controlled object. The performance index is expressed by the transfer function H_∞:

$$J = \inf \|P(s)\|_\infty \tag{31}$$

In the formula, J is performance indicators; $P(s)$ is transfer function matrix including actual objects and weighting functions, etc.

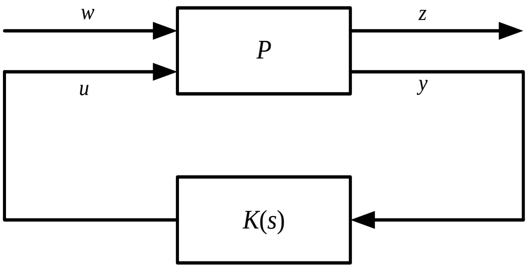

Figure 3. Standard H_∞ control problem

In the figure, P is the controlled object; $K(s)$ is the feedback controller; w is the external input signal; u is the control input signal; z is the control quantity; y is the output signal.

Suppose the state space realization of the transfer function $P(s)$ is obtained by formula (32):

$$\begin{aligned} \dot{x} &= Ax + B_1 w + B_2 u \\ z &= C_1 x + D_{11} w + D_{12} u \\ y &= C_2 x + D_{21} w + D_{22} u \end{aligned} \tag{32}$$

In the formula, x is the state variable.

Formula (32) can also be expressed as:

$$P(s) = \begin{bmatrix} P_{11} & P_{12} \\ P_{21} & P_{22} \end{bmatrix} = \begin{bmatrix} A & B_1 & B_2 \\ C_1 & D_{11} & D_{12} \\ C_2 & D_{21} & D_{22} \end{bmatrix} \tag{33}$$

Block $P(s)$ and H_∞ performance objective function formula (31) are combined as:

$$P(s) = \begin{bmatrix} P_{11} & P_{12} \\ P_{21} & P_{22} \end{bmatrix} = \begin{bmatrix} W_1 & -W_1 G \\ 0 & W_2 G \\ I & -G \end{bmatrix}$$
$$= \begin{bmatrix} A_{W1} & B_{W1}C_G & B_{W1} & 0 \\ 0 & A_G & 0 & B_G \\ C_{W1} & 0 & 0 & 0 \\ 0 & C_{W2} & 0 & I \\ 0 & C_G & I & 0 \end{bmatrix} = \begin{bmatrix} A & B_1 & B_2 \\ C_1 & D_{11} & D_{12} \\ C_2 & D_{21} & D_{22} \end{bmatrix} \tag{34}$$

In the formula, W_1 and W_2 are weighting functions; G is the state space realization of the transfer function.

The idea of robust control is to transform the performance and stability requirements of the system into the constraints of low frequency and high frequency of the closed loop transfer function. Because it is impossible to simultaneously satisfy the sensitivity index and robust stability in the full frequency domain, it is necessary to coordinate and optimize the two performance index parameters. Therefore, an optimization index with simultaneous weighting of performance and stability is proposed, that is, to seek the infinitesimal norm of controller K to stabilize G to satisfy the inequality. [33]:

$$\left\| \begin{matrix} W_1 S(s) \\ W_2 (I - S(s)) \end{matrix} \right\|_\infty \le 1 \tag{35}$$

In the formula, $S(s)$ is the sensitivity function.

Among them, the sensitivity function is:

$$S(s) = (I - (G(s)K(s)))^{-1} \tag{36}$$

The selection principle of weighting function is as follows:

1. Decrease sensitivity in middle and low frequency region. Due to the existence of target input and interference spectrum in the middle and low frequency bands, the sensitivity characteristics are greatly affected, so the sensitivity reduction processing is carried out in the middle and low frequency bands.
2. Increase sensitivity in high frequency region. In the high frequency region, due to the bad model accuracy and sensor noise, the robust stability is greatly affected, and the sensitivity increment is increased to improve the anti-high frequency noise characteristics and stability.

According to the above selection principle, weighting functions W_1 and W_2 are selected according to the characteristics of ABS control system. The robust control weighting function W_2 is the model error bound, so the definition of W_2 should be defined according to the error shape. According to the analysis of the wheel dynamics equation, it is concluded that it is a first-order inertial link, and the error transfer function of the model does not decrease in the high frequency region when the parameters have errors. In order to make the parameters change in a certain range, $W_2^{-1}=10(s/100+1)/(s+1)$ is selected according to the simulation practice. According to the ABS control principle based on slip rate, the ABS control system requires the output slip rate to track the expected slip rate, and the step response of the system error is required to asymptotically approach zero. Therefore, when selecting W_1, the sensitivity function is guaranteed to be as small as possible. In addition, the requirements of W_1 and W_2 are in conflict, so the relationship between the two functions should be coordinated, and $W_1^{-1}=(s+1)/(s/100+1)$ is selected.

In this paper, the MATLAB robust control box is used to solve the H_∞ robust control, and the mksys () and augtf () functions in the robust control box are used to establish variables describing the system and turn the augmented transfer function model into a standard H_∞ control problem. The optimal H_∞ control problem is solved by using the hinpof () function. This article takes a certain type of car as the research object, and the vehicle structure parameters are shown in Table 1.

According to the above analysis and the state equation of anti-lock system, the H_∞ robust controller is solved by using hinfpof command in MATLAB software, and the result is a fourth-order model.

By building the vehicle model, braking system, and road recognition module in MATLAB/Simulink, the H_∞ robust controller is finally used to control the ABS system. The control principle is shown in Figure 4.

Table 1. Vehicle Structure Parameters

Parameters and symbols	Numerical value/unit
Vehicle mass m	1764 kg
Sprung mass m_s	1646 kg
The distance from the center of mass to the front axis a	1.09 m
The distance from the center of mass to the back axis b	1.53 m
Vehicle wheelbase of front and rear T_f, T_r	1.535 m
Tire radius R_w	0.35 m
Height of the center of mass h	0.30 m
Moment of inertia of sprung mass around X axis I_x	288 $kg{\cdot}m^2$
Moment of inertia of wheel and its components I_ω	2400 $kg{\cdot}m^2$
Moment of inertia of sprung mass around the Z axis I_z	1353 $kg{\cdot}m^2$
Longitudinal stiffness of tire C_x	70000 $N{\cdot}m/rad$
Lateral stiffness of tire C_y	55000 $N{\cdot}m/rad$
Suspension roll damping C_ϕ	4000 $N{\cdot}m{\cdot}s/rad$
Suspension roll stiffness K_ϕ	50000 $N{\cdot}m/rad$

$$K(s)=\frac{-3.623s^{\wedge}4+1.124\times10^{6}s^{\wedge}3+3.975\times10^{7}s^{\wedge}2+1.886\times10^{8}s+2.406\times10^{8}}{s^{\wedge}4+2.263\times10^{4}s^{\wedge}3+4.92\times10^{6}s^{\wedge}2+7.148\times10^{7}s+6.658\times10^{7}} \quad (37)$$

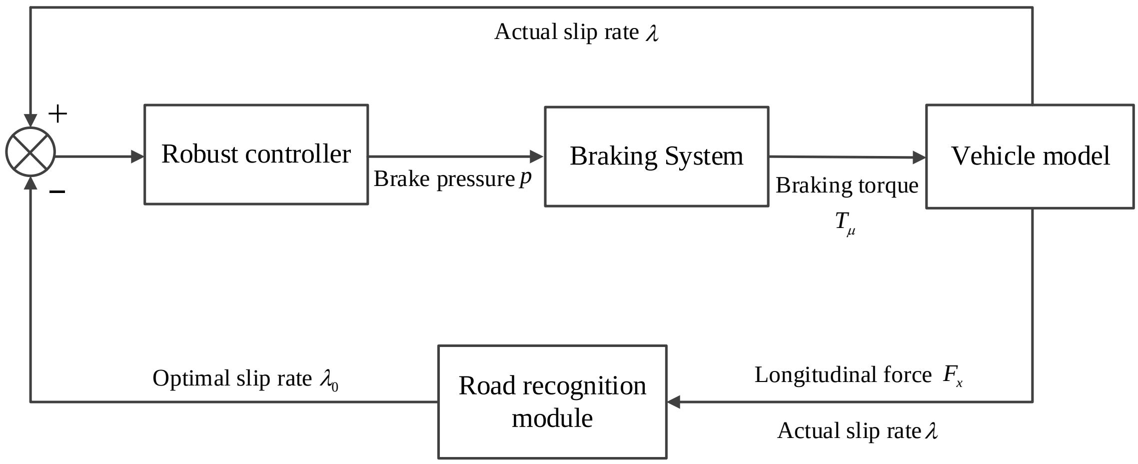

Figure 4. Schematic diagram of control system

4. Estimation of Road Adhesion Coefficient and Calculation of Optimal Slip Ratio

By analyzing the relationship between tire longitudinal force and slip rate, the adhesion coefficient of the road surface is determined. The Burckhardt tire longitudinal force model is selected as the research object, and various typical road surfaces are fitted through a large number of road tests $\mu-\lambda$ (adhesion coefficient-slip rate) relationship curve. The expression is given as [34]:

$$\mu(\lambda)=c_1\left(1-\exp\left(-c_2\lambda\right)\right)-c_3\lambda \tag{38}$$

In the formula, c_1, c_2 and c_3 are the fitting coefficients obtained from the experiment.

4.1. Design Road adhesion coefficient estimation based on fuzzy logic algorithm

Taking a single wheel as the road identification object, the longitudinal force F_x and slip rate λ of the tire are obtained by using the above eight-degree-of-freedom vehicle model and the Dugoff tire model. The longitudinal force F_x and slip rate λ are used as the input of the road identification module by using the fuzzy logic control to realize the identification of the current road.

1. Parameter fuzzification

It can be seen from Figure 5 that when the wheel slip rate is low, the discrimination of the road surface is low, and it is more difficult to identify the current road surface. When the slip rate is low, the identification of the road surface will not affect the work of the chassis safety system.

As shown in Figure 5, the slip rate is fuzzified into two fuzzy subsets [0,0.01) and (0.01,1]. When the slip rate is greater than 0.16, the membership degree of the fuzzy subset of the large slip rate is 1. According to experience, the tire longitudinal force is normalized and blurred, as shown in Figure 6.

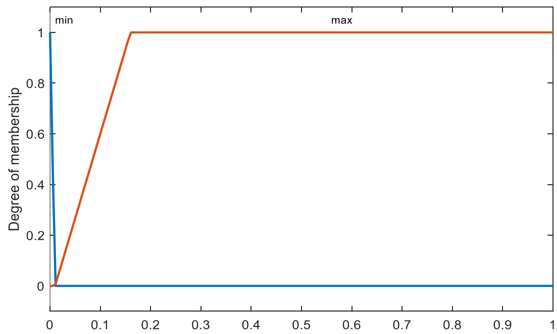

Figure 5. The fuzzification of wheel slip rate

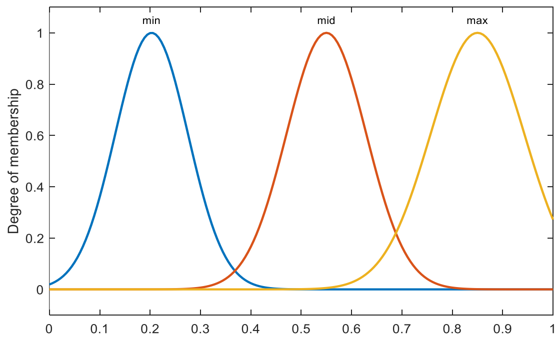

Figure 6. The fuzzy normalization of wheel longitudinal force

2. Fuzzy rulemaking

The identification results are continuously adjusted to make them consistent with the actual situation. The fuzzy rules are shown in Table 2. The fuzzy wheel slip rate and the normalized and fuzzy wheel longitudinal force are taken as the input of the fuzzy inference system, and the fuzzy weights coefficients c_1, c_2 and c_3 are outputs.

Table 2. Fuzzy rule table

Rule	Input		output		
	λ	F_x	c_1	c_2	c_3
1	min	none	max	min	max
2	max	min	min	max	min
3	max	mid	mid	mid	mid
4	max	max	max	min	max

3. Clarification

After the wheel slip rate and longitudinal force are blurred, they need to be cleared to get the desired output. Using the advantages of Gaussian membership function, the output weight coefficient is given better resolution. Combined with Figure 7, the center of gravity method is used to clarify the amount of blur [35].

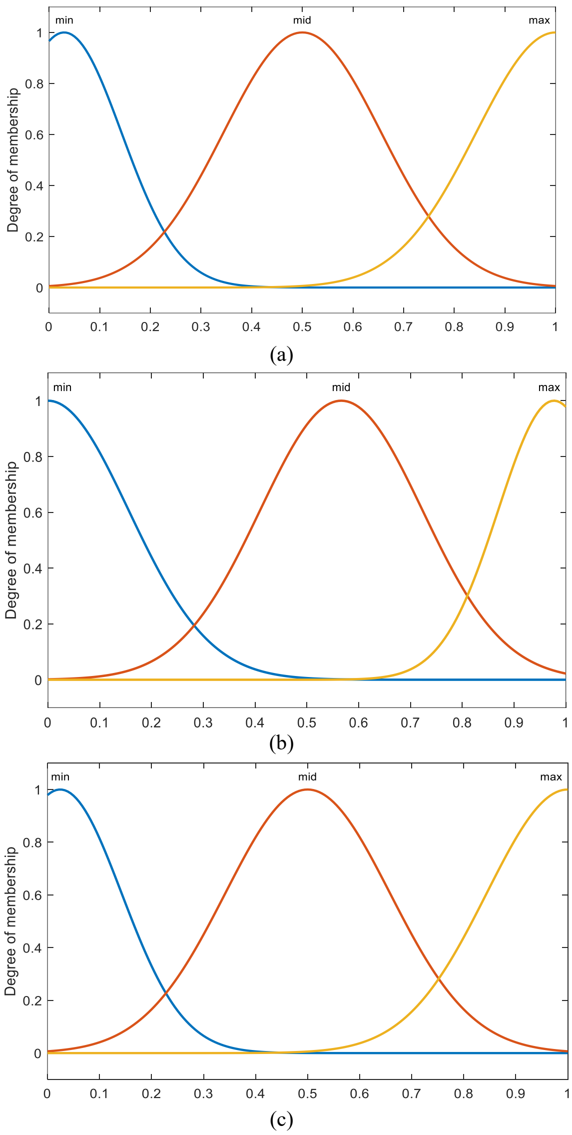

Figure 7. Clarifying fuzzy subsets and membership functions

4.2. Calculation of Optimal Slip Ratio

According to equation (38), let $\partial\mu/\partial\lambda = 0$, and get the optimal slip rate:

$$\lambda_0 = \frac{1}{c_2}\ln\frac{c_1c_2}{c_3} \tag{39}$$

In the formula, λ_0 is the optimal slip rate; c_1, c_2 and c_3 are the weight coefficients obtained by fuzzy logic algorithm.

5. Simulation Results and Analysis

5.1. Simulation Results and Analysis of Robust Control

This paper selects a certain type of car as the research object, and the vehicle structure parameters are described in Table **1** above. The test condition selects a road with a road adhesion coefficient of $\mu = 0.8$, and the vehicle speed is set to 80 *km/h*. The simulation model of ABS is established by Matlab / Simulink software platform, and the obtained $K(s)$ is used as the robust controller of ABS to simulate, and the dynamic response of the system is obtained. The simulation results are shown in Figure 8-10.

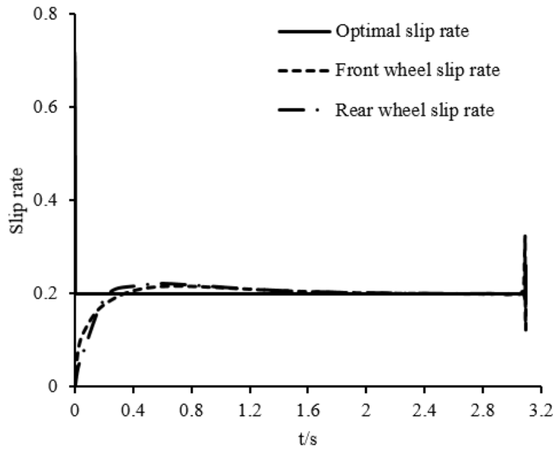

Figure 8. Slip rate curve

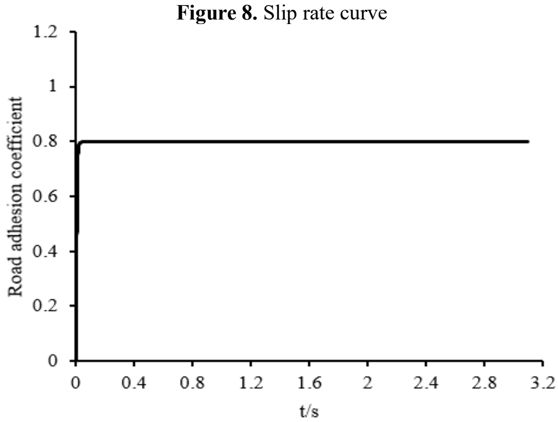

Figure 9. Road adhesion coefficient

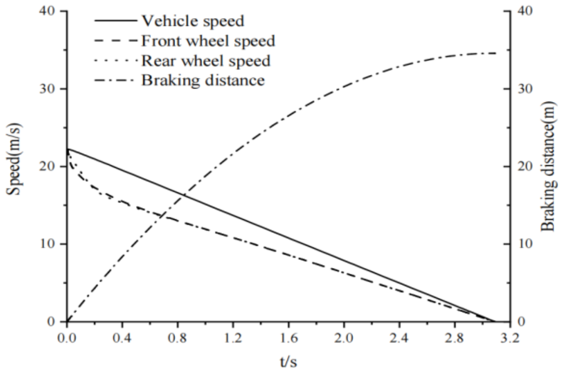

Figure 10. Robust control of vehicle speed, wheel speed, and braking distance curve

According to Figure 8, the wheel slip rate basically changes around the optimal slip rate, indicating that the front and rear wheels can make full use of the maximum ground adhesion to improve the braking performance, so that the car can stop within the shortest distance. According to Figure 9, it shows that the road surface recognition module can accurately estimate the current road surface adhesion coefficient and has a better control effect. As shown in Figure 10, after the ABS system is used, the vehicle speed and wheel speed are constantly decreasing, and finally reduced to 0 at the same time, indicating that the wheels are locked when the vehicle brake stops, which improves the handling stability in the braking process. According to the national passenger vehicle braking standard, when the braking speed is $80km/h$, the braking distance needs to meet $\leq 50.7m$. According to the braking distance curve, when the braking speed is $80\,km/h$, the braking distance is $34.56m \leq 50.7m$,which meets the national standard.

5.2. Simulation Comparative Analysis of Traditional PID Control and Robust Control

Traditional PID algorithm is a widely used and mature control method. It does not need to understand the mathematical model of the controlled object, as long as the parameters are adjusted online according to the system situation, and the appropriate proportional, integral and differential coefficients are matched [36]. The simulation model of ABS is established by MATLAB/Simulink software platform. Based on the traditional PID algorithm, the dynamic response of the system is obtained. The simulation results are shown in Figure 11-14.

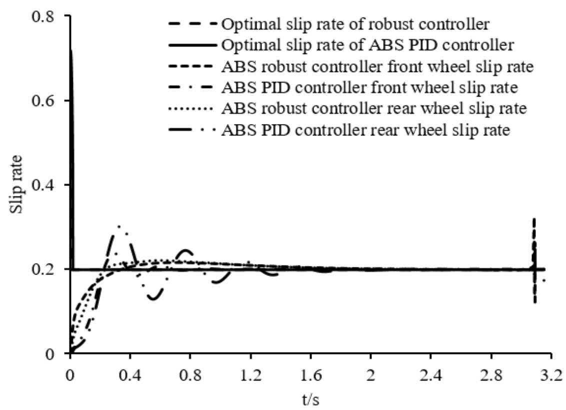

Figure 11. Slip rate curve

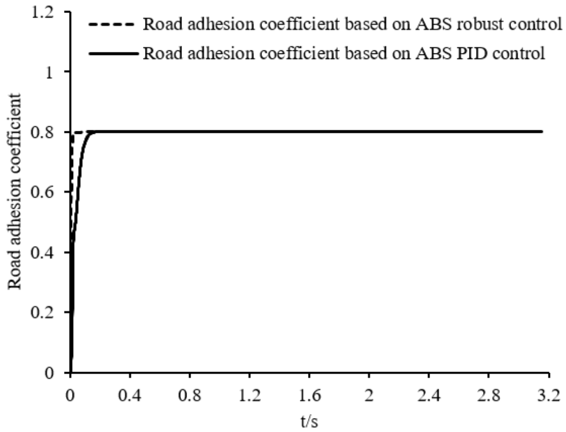

Figure 12. Road adhesion coefficient

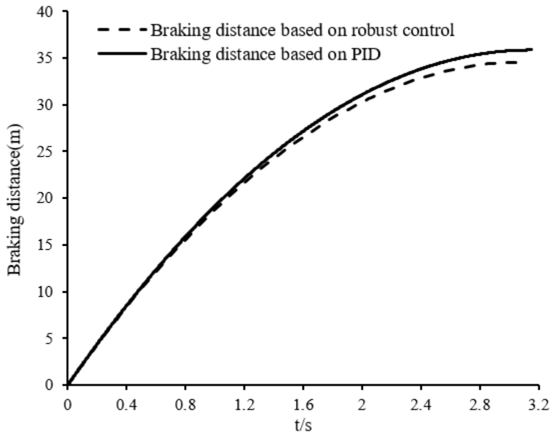

Figure 13. Braking distance curve

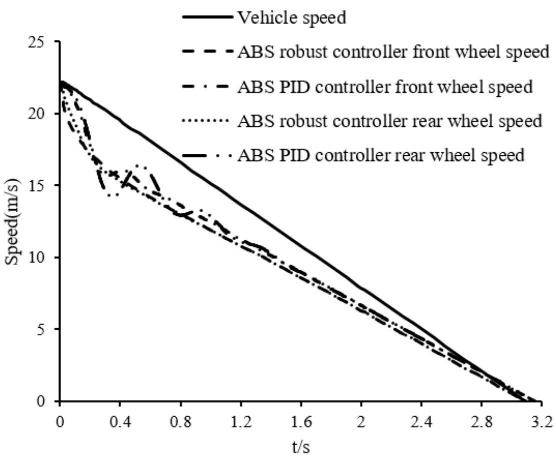

Figure 14. Vehicle speed and wheel speed curve

According to the simulation results in Figure 11 and 12, Wheel slip rate of ABS system based on the traditional PID control algorithm basically changes near the optimal slip rate, and the road surface identification module can accurately estimate the road surface adhesion coefficient, which has a good control effect. According to Figure 13, the braking distance satisfies $\leq 50.7m$ and meets the national standard.

Table 3. Braking effect

control arithmetic	Braking time (s)	Braking distance (m)
Traditional PID controller	3.15	35.99
Robust controller	3.09	34.56

As can be seen from Figure 11-13 and Table 3, when the robust controller works, the car stops at 3.09 *s* and the braking distance is 34.56 *m*. When the traditional PID controller is used, the car stops at 3.15 *s* and the braking distance is 35.99 *m*. According to Figure 14, the change curve of speed and wheel speed based on traditional PID control are not as smooth as that of robust control. In terms of control accuracy, response time and robust stability, the robust controller is more superior than the traditional PID controller. The robust controller can ensure that the car completes the braking process with shorter braking distance and less braking time, and the safety factor is higher

6. Conclusion

In this paper, the robust ABS controller based on road surface recognition is designed. The adhesion coefficient of road surface is estimated by fuzzy logic control method to realize road surface recognition, and the optimal slip rate is obtained dynamically. According to the obtained dynamic slip rate, the robust controller of ABS is designed. Compared with the traditional PID control ABS system, the ABS system based on robust control can control the wheel slip rate near the optimal slip rate, make full use of the maximum ground adhesion, and obtain sufficient ground brake force. The robust controller can ensure that the car completes the braking process with a shorter braking distance and braking time, with higher safety factor, rapid response, better robustness and stability, and the overall control effect is better than PID control. Therefore, it can provide a theoretical reference for the actual ABS control system.

Acknowledgements

This research was supported by the Key scientific and technological project of Henan Province (No. 172102210022, No.182102210086), Natural Science Foundation of Henan Province of China (No.182300410265), and National Undergraduate Training Program for Innovation and Entrepreneurship (No. 201810460069).

References

[1] Wu J, Liu YH, Wang FB, Bao CJ, Sun Q, Zhao YQ. Vehicle active steering control research based on two-DOF robust internal model control. Chinese Journal of Mechanical Engineering,2016, 29(04),739-746.

[2] Chen J, Song J, Li L, Ran X, Jia G, Wu KH. A novel pre-control method of vehicle dynamics stability based on critical stable velocity during transient steering maneuvering. Chinese Journal of Mechanical Engineering, 2016, 29 (03), 475-485.

[3] Zhao ZX, Fan XB, Jin K, Wang F. Simulation study of ABS Fuzzy control based on road surface recognition. Laboratory science,2017,20(05):75-80.
[4] Hu K. Research on Air Pressure ABS Control Algorithm Based on Threshold Logic. MSc Dissertation, Hunan University, Changsha, China, May 2013.
[5] Li G, Wang Y, Zhao DY. Study on Control Strategy and Experiment of Automobile ABS Based on Logical Threshold. Modern Manufacturing Engineering, 2017, (07):12-16.
[6] Wu L, Sun Y, Sun YR. Modeling and Simulation of Automobile ABS System Based on Matlab/Simulink. Sensor Detection and Internet of Things,2014,(5):75-80.
[7] Ammar A. Design of neuro-fuzzy self-tuning PID controller for antilock braking systems. Journal of Babylon University/Engineering Sciences,2014,22(4):775 -787.
[8] Ma ZW, Ni LQ, Chen YK, Zhang HQ, Lin F. Research on ABS Control Strategy Based on Neuro-fuzzy PID. Journal of Chongqing University of Technology (Natural Science), 2018, 32 (09):14-22.
[9] Liu J, Du TH, He LL, Xu DB. Fuzzy Neural Network Model Reference Adaptive Control Strategy in Automobile ABS. Automotive Electrical Appliances,2006,(01):4-7.
[10] Okyay A, Cigeroglu E, Baslama SC. A new sliding-mode controller design methodology with derivative switching function for anti-lock brake system. Journal of Mechanical Engineering Science, 2013,227 (11): 2487-2503.
[11] Leng X. Research on Automobile Anti-lock Braking System Based on Sliding Mode Variable Structure. MSc Dissertation, Harbin University of Science and Technology, Harbin, China, March 2009.
[12] Wang JS, Yang XD. Self-seeking Optimal Control of Automobile Anti-lock Braking System. J Automotive Engineering,2004,(03):299-301.
[13] Li WJ, Fu TL, Chen FL, Wang XD. Self-seeking Optimal Control of Automobile Antilock Braking System. Journal of Harbin University of Science and Technology, 2010, 15 (05):27-30+39.
[14] Fu YM, Liu WY. Design of a special vehicle ABS system based on adaptive fuzzy PID control. Guizhou Science, 2021, 39 (02): 91-97.
[15] Emam, A.S., Mohamed, E.S. Enhancement of Anti-locking Brake System Performance by using Intelligent Control Technique with Different Road Conditions[J]. International Journal of Vehicle Structures and Systems,2021,13(1) 37-45.
[16] Xu YF. Research and optimization of anti-lock braking system for new energy vehicles. Microcomputer Applications,2021,37(03):124-127.
[17] He JD, Zheng YJ, Tan Y, Wu G. Research on Vehicle Anti-braking System Control Algorithm Based on Fuzzy Immune Adaptive PID Control. Third International Conference on Digital Manufacturing & Automation. IEEE Computer Society. Guilin, China (2012)
[18] Jia HN, Yao JX. Research on ABS simulation based on adaptive Fuzzy PID control. Automobile Practical Technology, 2020,(03):147-151.
[19] Mao XW, Li GJ. Research on vehicle anti-lock braking system based on Fuzzy immune PID control. Journal of Jiangsu University of Technology,2020,26(04):95-102.
[20] Yao F, Lin XH, Wu ZB, Li GQ, Jiang F. Research on auto disturbance rejection control of automobile anti-lock braking system. China Journal of Highway and Transport, 2021, 34(03):235-244.
[21] Wang GW, Yin AD. Research on ABS control of electric vehicles based on neural network road recognition. Journal of Hefei University of Technology (Natural Science Edition) ,2020,43(07):878-883.
[22] Shen C, Hui YL, You YC. Optimal control of automobile anti-lock braking system. Journal of Liaoning Transportation College,2005,(02):59-61.
[23] Wu MX. Optimal Tracking Control of Slip Ratio of Anti-lock Braking System for High-speed Vehicles under Complex Road Conditions. Journal of Shanghai Normal University (Natural Science Edition) ,2019, 48(04):375-382.
[24] Wang F, Fan XB, Zhang YM, Jin K, Yang F. Fuzzy identification based on tire/road adhesion feature. Computer Aided Drafting, Design and Manufacturing,2015,25(01):62-67.
[25] Peri S, Anti D, Miti D, Milojkovi M. Generalized quasi-orthogonal polynomials applied in sliding mode-based minimum variance control of ABS. Acta Polytechnica Hungarica,2020,17(4):165-182.
[26] Chereji E, Radac MB, AI SS. Sliding Mode Control Algorithms for Anti-Lock Braking Systems with Performance Comparisons. Algorithms,2020,14(1):2.
[27] Wang JC, He R. Hydraulic anti-lock braking control strategy of a vehicle based on a modified optimal sliding mode control method. Proceedings of the Institution of Mechanical Engineers, Part D: Journal of Automobile Engineering. 2019, 233 (12): 3185-3198.
[28] Wanaskar V, Shendge P, Phadke S. A disturbance observer-based sliding mode control for anti-lock braking system. 2019 Second International Conference on Advanced Computational and Communication Paradigms (ICACCP), Lanzhou China (2019).
[29] Hossein M. Robust predictive control of wheel slip in anti-lock braking systems based on radial basis function neural network. Applied Soft Computing,2018,70:318-329.
[30] Yu HX. Research on Intelligent Vehicle Collision Avoidance Based on State Estimation. PhD Dissertation, Beijing University of Technology, Beijing, China, June 2015.
[31] Wang B, Sun RY. Research on road surface recognition method based on state characteristic factors. Automotive Engineering,2012,34(06):506-510+522.
[32] Liu XY. Research on Vehicle Stability Based on Direct Yaw Torque Control. PhD Dissertation, Hefei University of Technology, Hefei, China, November 2010.
[33] Chen J. Theory and Practice of Automobile Anti-lock Braking System. 1st ed. Beijing Institute of Technology Press: Beijing,1999.
[34] Wang B, Sun RY, Xu YH, Wu LD. Road surface recognition method considering road unevenness. Chinese Journal of Mechanical Engineering,2012,48(24):127-133.
[35] Abdalla M O, Al-Jarrah T M. Fuzzy Logic Control of an Electrical Traction Elevator. Jordan Journal of Mechanical and Industrial Engineering, 2011,5(1):97 -106.
[36] Rajagopal, Kalaivani, Ponnusamy, Lakshmi. Hybrid DEBBO Algorithm for Tuning the Parameters of PID Controller Applied to Vehicle Active Suspension System.Jordan Journal of Mechanical and Industrial Engineering,2015,9(2):85-102.